Applied Mathematical Sciences, Vol. 17, 2023, no. 13, 615 - 623
HIKARI Ltd, www.m-hikari.com
https://doi.org/10.12988/ams.2023.918515

On the Chaotic Dynamics of a Modified Nosé-Hoover Oscillator

Bo Deng

Department of Mathematics
University of Nebraska-Lincoln, USA

Jorge Duarte

ISEL-Engineering Superior Institute of Lisbon
Department of Mathematics
Rua Conselheiro Emídio Navarro 1, 1949-014 Lisboa, Portugal
and Center for Mathematical Analysis, Geometry and Dynamical Systems
Mathematics Department, Instituto Superior Técnico
Universidade de Lisboa, Av. Rovisco Pais 1, 1049-001 Lisboa, Portugal

Cristina Januário

ISEL-Engineering Superior Institute of Lisbon
Department of Mathematics
Rua Conselheiro Emídio Navarro 1, 1949-014 Lisboa, Portugal
and Center for Research and Development in Mathematics and Applications, (CIDMA)
Department of Mathematics, University of Aveiro, 3810-193 Aveiro, Portugal

Nuno Martins

Mathematics Department and Center for Mathematical Analysis,
Geometry and Dynamical Systems
Instituto Superior Técnico, Universidade de Lisboa
Av. Rovisco Pais 1, 1049-001 Lisboa, Portugal

Abstract

This article reports on a study of the two-dimensional parameter space of a generalized time-reversible Nosé-Hoover oscillator. Instead of considering its original form, whose study of the one-dimensional parameter space has recently received new insights, we examine the Nosé-Hoover model slightly modified by using a new parameter ϵ to introduce a dissipative term to its energizing-damping variable. We use the maximum Lyapunov exponent to numerically characterize the chaotic dynamics of the model, at representative points of the two-dimensional parameter space, treating separately two dynamical regimes resulting from: (i) the effect of lower values of ϵ and (ii) the effect of higher values of ϵ. It is shown that, for higher values of the new dissipative parameter ϵ, the existence of chaotic behavior only prevails for the backwards dynamics.

Mathematics Subject Classification: Primary 34A34; Secondary 97M10, 97M50

Keywords: Modified Nosé-Hoover oscillator, Nonlinear differential equations, chaotic dynamics

1 Introduction and preliminaries

In spite of their importance in nonlinear dynamics theory, the topological structures of phase trajectories and the mechanisms of the emergence of chaos, in time-reversible dynamical systems, haven't been a subject of intense research. To the extent of our knowledge, only a few problems have been addressed in order to enhance our understanding of the consequences of the Nosé's work for time-reversible flows (see, for instance, [1], [2], [3], [4], [5], [6], and references therein). In the context of nonlinear systems, when both the backwards and forwards dynamics are satisfied by the same equations subject to only some sign changes of phase variables, these equations are called time-reversible equations.

In his seminal work published in 1984 (please see [7] and [8]), Shiuchi Nosé presented a set of equations that gave rise to a new paradigm in the study of thermodynamics. In [1], it is shown an interesting review about the study of Nosé-Hoover oscillator throughout the years, its meaning and connections with other fields in an interdisciplinary context. After studying the Nosé's equations, Hoover and his collaborators, Posh and Vesely, obtained in 1986 the Nosé-Hoover oscillator with the following equations of motion (please see [9] and [10])

$$\dot{x} = y; \;\; \dot{y} = -x - yz; \quad \dot{z} = \alpha \left(y^2 - 1 \right). \tag{1}$$

This system models the one-dimensional harmonic oscillator, obtained using Nosé's canonical equations of motion, where x represents the oscillator coordinate, the variable y represents momentum and the variable z represents the friction coefficient.

Given the time-reversible property of the one-parameter Nosé-Hoover equations, one question naturally appears: how different is the impact of a second parameter on the backwards and forwards dynamics of time-reversible systems? This question is justified by the possibility of computing different measures of complexity. In a very recent work [11], we analyzed the effect of a singular parameter, present in the equations of the simple Nosé-Hoover oscillator, on the backwards and forwards dynamical behavior by the computation of the spectrum of Lyapunov exponents. Adopting a comparative backwards/forwards approach, we have identified different chaotic scenarios, estimated the predictability of attractors and determined their fractal dimension.

The findings reported in the present paper consider a generalized Nosé-Hoover oscillator [12], namely the two-parameter, three-dimensional set of nonlinear first-order ordinary differential equations given by

$$\dot{x} = y; \;\; \dot{y} = -x - yz; \quad \dot{z} = \alpha \left(y^2 - 1 - \epsilon z\right), \tag{2}$$

which differs from the original form of the Nosé-Hoover oscillator (1) by the small dissipative term added to the energizing-dapping variable z, which includes the parameter ϵ. As a consequence, there are two parameters present in (2), namely α and ϵ. Here, the simultaneous variation of these two parameters will be considered to investigate the eye-catching and noteworthy dynamical features in the two-dimensional (α, ϵ)-parameter space of the modified time-reversible Nosé-Hoover oscillator (2). Other studies regarding modifications of the Nosé-Hoover oscillator can be find, for instance, in [4].

Due to the absence of explicit solutions for these type of systems, our study mainly depends on numerical simulations, which have been obtained using MATHEMATICA 13.0, *NDSolve StiffnessSwitching method* with *Machine-precision* corresponding to 16 digits of mantissa and *MaxStepSize* 10^{-9}. Having stated this, throughout our study we will consider the fixed initial conditions $x(0) = 0.9209$, $y(0) = -0.1560$ and $z(0) = 0.9179$, inside the attractor without transient dynamics. Our studied (α, ϵ)-parameter space is divided in two subspaces

$$L_\epsilon = \left\{(\alpha, \epsilon) \in \mathbb{R}^2 : 0 \leq \alpha \leq 14 \wedge 0 \leq \epsilon \leq 0.00012\right\}$$

and

$$H_\epsilon = \left\{(\alpha, \epsilon) \in \mathbb{R}^2 : 0 \leq \alpha \leq 14 \wedge 0.00012 < \epsilon \leq 0.05\right\}.$$

For illustrative purposes only, taking a particular pair of parameter values $(\alpha, \epsilon) \in L_\epsilon$, $(\alpha, \epsilon) = (11, 0.00002)$, Fig.1 provides us with a direct comparison

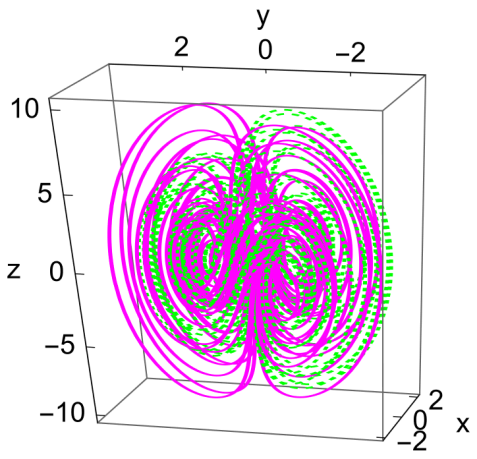

Figure 1: Joint presentation of the backwards and forwards dynamics of the modified time-reversible Nosé-Hoover oscillator - Backwards trajectory in dashed green and forwards trajectory in continuous pink. We exhibit the 3D-attractor, taking $t \in [-90, 0]$, $t \in [0, 90]$, $\alpha = 11$ and $\epsilon = 0.00002$.

between attractors of the system's backwards/forwards phase-space trajectories (backwards - corresponding to the dashed green trajectories and forwards - corresponding to the continuous pink trajectories). As a matter of fact, the backwards and forwards dynamics do not coincide and different topological structures emerge in the phase-spaces.

2 A global view of the (α, ϵ)-parameter space: the effect of ϵ and time-reversible chaos

In this section, the two (α, ϵ)-parameter spaces, L_ϵ and H_ϵ, are interpreted using: (i) the maximum Lyapunov exponent and (ii) selected bifurcation diagrams to characterize the chaotic dynamics of the generalized oscillator (2). In order to achieve this goal, two subsections are considered, treating separately two dynamical regimes resulting from: the effect of lower values of ϵ (Subsection 2.1) and the effect of higher values of ϵ (Subsection 2.2).

As established in the literature, Lyapunov exponents are used to characterize the *dynamics* of chaotic attractors. In this section, we estimate the spectrum of Lyapunov exponents of the modified Nosé-Hoover oscillator and use the maximum of these values to identify regions of the (α, ϵ)-parameter space corresponding to chaotic behavior.

Lyapunov exponents are taken as a valuable indicator of the exponential divergence of infinitesimally close trajectories in the phase space, characteristic

of the chaotic attractors. For a simple description of the Lyapunov exponents, as a quantitative measure of the rate of separation of initially close points, as well as the use of an effective computation method, please see our previous work [11], and references therein.

As established in the literature, the chaotic behavior is associated with a positive *maximum Lyapunov exponent* $\lambda_{\max}$. More precisely, based on the values of the first and the second Lyapunov exponents, different dynamical regimes can be identified. Some of these regimes are presented in the following table.

$\mathbf{1}^{st}$ **Lyap**	$\mathbf{2}^{nd}$ **Lyap**	**Behavior**
> 0	$= 0$	Chaotic
$= 0$	$= 0$	Quasi-periodic
$= 0$	< 0	Periodic

2.1 The parameter space L_ϵ and the dynamical effect of lower values of ϵ

Given the previous dynamical considerations, in Fig.2, we provide a characterization of the complexity for the system (2), considering the (α, ϵ)-parameter space L_ϵ, for which $0 \leq \epsilon \leq 14$ and $0 \leq \epsilon \leq 0.00012$. In particular, Fig.2 (Upper panel) displays two pictures providing the variation of the maximum Lyapunov exponent $\lambda_{\max} = \lambda_1$, respectively with the backwards and forwards dynamics. Directly related to the dashed line represented on these pictures, the Fig.2 (Lower panel) gives insights about the long time behavior of variable x, by representing bifurcation diagrams obtained from the successive local maxima of x, for $\epsilon = 0.00002$ and taking $\alpha \in [0, 14]$ as bifurcation parameter. It is useful to notice that the chaotic windows of these bifurcation diagrams confirm the existence of the parameter sections, of the represented straight line, for which the respective trajectories in the parameter space are chaotic.

2.2 The parameter space H_ϵ and the dynamical effect of higher values of ϵ

Inspired by the numerical results of the previous paragraph, in Fig.3 we provide a characterization of the complexity for the system (2), this time corresponding to the (α, ϵ)-parameter space H_ϵ, corresponding to with higher values of ϵ, $\epsilon > 0.00012$. Interestingly, the existence of chaotic behavior only prevails for the backwards dynamics. Particularly, on the upper panel, the variation of the maximum Lyapunov exponent is considered, for the mentioned backwards dynamics, taking $0 \leq \alpha \leq 14$ and $0.00012 < \epsilon \leq 0.05$. Directly related to the dashed horizontal line $\epsilon = 0.02$ represented on this picture, the Fig.3 (Lower panel) gives insights about the long time behavior of variable x, by

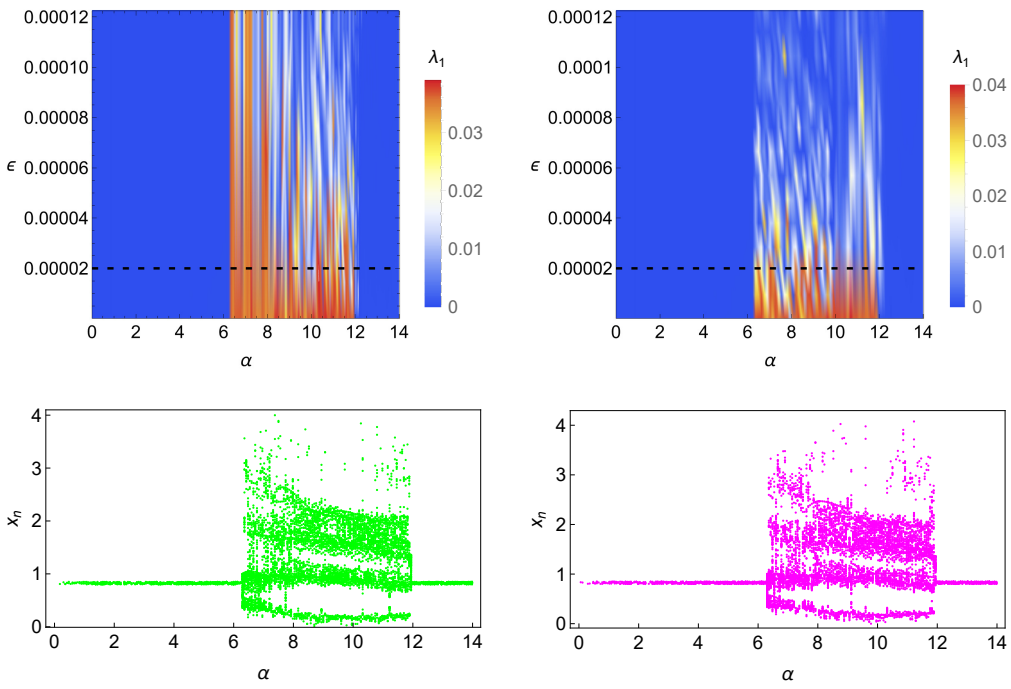

Figure 2: Numerical characterization of the dynamics for the modified Nosé-Hoover oscillator corresponding to the (α, ϵ)-parameter space L_ϵ, with low values of ϵ, $\epsilon \leq 0.00012$. Upper panel - Variation of the maximum Lyapunov exponent in L_ϵ, for which $0 \leq \alpha \leq 14$ and $0 \leq \epsilon \leq 0.00012$: backwards dynamics (left) and forwards dynamics (right). Lower panel - Bifurcation diagrams for points (α, ϵ) along the horizontal dashed straight line $\epsilon = 0.00002$ represented on the upper panel ($\epsilon = 0.00002$ and $\alpha \in [0, 14]$): backwards dynamics (left) and forwards dynamics (right).

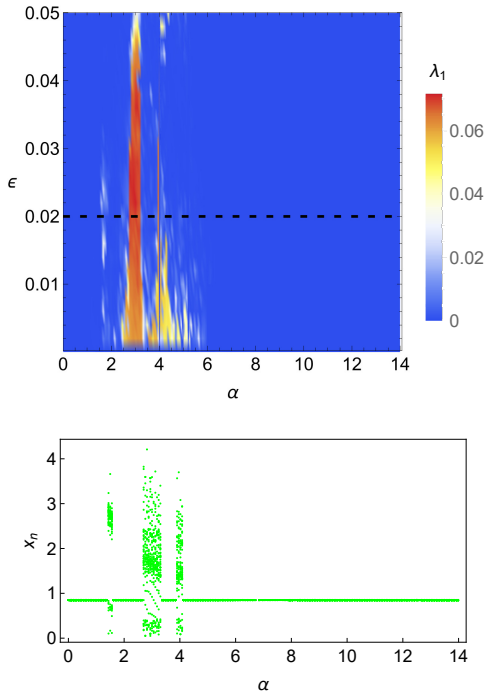

Figure 3: Numerical characterization of the dynamics for the modified Nosé-Hoover oscillator corresponding to the (α, ϵ)-parameter space with higher values of ϵ ($\epsilon > 0.00012$). The existence of chaotic behavior only prevails for the backwards dynamics. Upper panel - Variation of the maximum Lyapunov exponent, for the mentioned backwards dynamics, taking $0 \leq \alpha \leq 14$ and $0.00012 < \epsilon \leq 0.05$. Lower panel - Bifurcation diagram for points (α, ϵ) along the horizontal dashed straight line $\epsilon = 0.02$, represented on the upper panel ($\epsilon = 0.02$ and $\alpha \in [0, 14]$).

representing a bifurcation diagram obtained from the successive local maxima of x, for $\epsilon = 0.02$ and taking $\alpha \in [0, 14]$ as bifurcation parameter. As expected, the chaotic windows of this bifurcation diagram confirm the existence of the parameter sections, of the represented straight line, for which the respective trajectories in the parameter space are chaotic.

2.3 Final considerations

In this paper, numerical simulations have been performed on a two-dimensional parameter space of the modified Nosé-Hoover oscillator. The parameter spaces considered display different dynamical regimes, particularly chaotic and periodic structures. Curiously, for higher values of ϵ, $\epsilon > 0.00012$, the existence of chaotic behavior only prevails for the backwards dynamics.

We emphasize that for parameter regions whose related parameters generate chaotic trajectories in the phase-space, the first (maximum) Lyapunov exponent is greater than zero, while the second Lyapunov exponent is equal to zero. For parameters resulting in periodic trajectories in the phase space, the first (maximum) Lyapunov exponent and the second Lyapunov exponent are respectively zero and less than zero.

Acknowledgments. This research was partially supported by FCT/Portugal through CAMGSD, IST-ID, projects UIDB/04459/2020 and UIDP/04459/2020 (JD and NM). This work was also partially supported by the Portuguese Foundation for Science and Technology (FCT) within the projects UIDB/04106/2020 and UIDP/04106/2020 (CIDMA) (CJ).

References

[1] Julien Clinton Sprott, William Graham Hoover, Carol Griswold Hoover, Heat conduction and the lack thereof, in time-reversible dynamical systems: Generalized Nosé-Hoover oscillators with a temperature gradient, *Phys. Rev. E*, **89** (2014), 042914. https://doi.org/10.1103/physreve.89.042914

[2] L. Wang, X.-S Yang, The invariant tori of knot type and the interlinked invariant tori in the Nosé-Hoover oscillator, *Eur. Phys. J. B.*, **88** (2015a), 78. https://doi.org/10.1140/epjb/e2015-60062-1

[3] L. Wang, X.-S Yang, A vast amount of various invariant tori in the Nosé-Hoover oscillator, *Chaos*, **25** (2015b), 123110. https://doi.org/10.1063/1.4937167

[4] P. C. Rech, Quasiperiodicity and chaos in a generalized Nosé-Hoover oscillator, *Int. J. Bifurcation Chaos*, **26** (2016), 10. https://doi.org/10.1142/s0218127416501704

[5] J. Llibre, M. Messias, A. C. Reinol, Global dynamics and bifurcation of periodic orbits in a modified Nosé-Hoover oscillator, *Journal of Dynamical and Control Systems*, **27** (2021), 3. https://doi.org/10.1007/s10883-020-09491-5

[6] S. Cang, L. Wang, Y. Zhang, Z. Wang, Z. Chen, Bifurcation and chaos in a smooth 3D dynamical system extended from Nosé-Hoover oscillator, *Chaos, Solitons and Fractals*, **158** (2022). https://doi.org/10.1016/j.chaos.2022.112016

[7] S. Nosé, A unified formulation of the constant temperature molecular dynamics methods, *J. Chem. Phys.*, **81** (1984a), 511. https://doi.org/10.1063/1.447334

[8] S. Nosé, A molecular dynamics method for simulations in the canonical ensemble, *Mol. Phys.*, **52** (1984b), 255. https://doi.org/10.1080/00268978400101201

[9] W. G. Hoover, Canonical dynamics: equilibrium phase-space distributions, *Phys. Rev. A*, **31** (1985). https://doi.org/10.1103/physreva.31.1695

[10] H. A. Posch, W. G. Hoover, F. G. Vesely, Canonical dynamics of the Nosé oscillator: Stability, order, and chaos, *Phys. Rev. A*, **33** (1986). https://doi.org/10.1103/physreva.33.4253

[11] B. Deng, J. Duarte, C. Januário, N. Martins, Measures of Complexity in Nosé-Hoover Oscillator and a Possible New Chaos Generation Mechanism, *Applied Mathematical Sciences*, **17** (2023) no. 11, 517-534. https://doi.org/10.12988/ams.2023.917477

[12] Q. Han, B. Deng, X-S. Yang, The existence of ω-limit set for a modified Nosé-Hoover oscillator, *Discrete and Continuous Dynamical Systems Series B*, **27** (2022), 7275-7300. https://doi.org/10.3934/dcdsb.2022043

Received: August 7, 2023; Published: August 24, 2023